Optical Conductivity and Penetration Depth in MgB_2

A. V. Pronin,[1,2] A. Pimenov,[1,*] A. Loidl,[1] and S. I. Krasnosvobodtsev[3]

[1]*Experimentalphysik V, EKM, Universität Augsburg, 86135 Augsburg, Germany*
[2]*Institute of General Physics, Russian Academy of Sciences, 119991 Moscow, Russia*
[3]*P. N. Lebedev Physics Institute, Russian Academy of Sciences, 117924 Moscow, Russia*

(Received 17 April 2001; published 14 August 2001)

The complex conductivity of a MgB_2 film has been investigated in the frequency range $4 < \nu < 30\ \mathrm{cm}^{-1}$ and for temperatures $2.7 < T < 300$ K. The overall temperature dependence of both components of the complex conductivity is reminiscent of BCS-type behavior, although a detailed analysis reveals a number of discrepancies. A peak in the temperature dependence of the real part of the conductivity is detected for frequencies below $9\ \mathrm{cm}^{-1}$. The superconducting penetration depth follows a T^2 behavior at low temperatures.

DOI: 10.1103/PhysRevLett.87.097003 PACS numbers: 74.25.Gz, 74.25.Nf, 74.70.Ad, 74.76.–w

The recent discovery of superconductivity at relatively high temperature ($T_c \approx 39$ K) in a simple binary compound, magnesium boride [1], has stimulated extensive theoretical and experimental studies in this material. Most of these studies are attempting to find the pairing mechanism that leads to the superconductivity in this compound [2]. The strongest evidence for phonon-mediated superconductivity in MgB_2 comes from the boron-isotope effect measured by the Canfield group [3]. Further confirmation for such a mechanism would be an observation of characteristic features predicted by the BCS theory for different experimentally measured quantities, such as an s-wave superconducting gap in tunneling and optical experiments or a coherence peak in NMR and in the real part of the low-frequency conductivity. During the several months that passed after the discovery of superconductivity in MgB_2, large experimental efforts were undertaken to observe such features. However, the absence of high-quality samples hampers the collection of reliable experimental results. The tunneling data obtained on ceramic samples [4] confirm roughly the BCS predictions for a s-wave gap, although the ratio $2\Delta(0)/kT_c$ varies significantly from one report to another, being between 1.2 and 4. These variations together with some deviations from the temperature dependence of the BCS gap have mostly been explained by imperfections of the sample surface, but alternative explanations, e.g., based on multiple gaps, have also been proposed [5]. First photoemission data [6] could be successfully described using an isotropic s-wave gap with $2\Delta(0)/kT_c = 3$. However, the indication of a multiple gap in the photoemission spectra was also reported in subsequent investigations [7]. The NMR experiments [8] reveal a tiny coherence peak with $2\Delta(0)/kT_c = 5$, which indicates that a strong coupling regime dominates in MgB_2. The temperature dependence of the penetration depth, which is indicative of the gap symmetry, shows either quadratic (muon spin-rotation experiments [9]) or linear (H_{c2} measurements [10]) laws, both being inconsistent with an activated behavior, predicted by the BCS theory. Few optical studies have been reported till now [11,12]. The grazing reflectivity spectra demonstrated a gradual increase at frequencies below $70\ \mathrm{cm}^{-1}$ with a maximum about $25–30\ \mathrm{cm}^{-1}$, which might be considered as a sign of an anisotropic superconducting gap with a minimum value $2\Delta(0) = 3–4$ meV [11]. Infrared transmittance measurements [12] indicate an energy gap $2\Delta(0) = 5.6$ meV ($2\Delta/kT_c = 1.8$). Therefore, the experimental data are rather controversial, and there is no general agreement whether MgB_2 is a BCS-type superconductor or not.

In this paper we report on optical investigations of a high-quality MgB_2 film in the submillimeter frequency range ($4 < \nu < 30\ \mathrm{cm}^{-1}$). Both components of the complex conductivity $\sigma^*(\nu, T) = \sigma_1 + i\sigma_2$ have been directly measured as a function of temperature and frequency. This type of measurement has already been applied to a variety of high-temperature and conventional superconductors and has proven to be a powerful method for studying the electrodynamical properties of these materials [13].

The MgB_2 film was grown by two-beam laser ablation [14] on a plane-parallel sapphire substrate $10 \times 10\ \mathrm{mm}^2$ in size. The crystallographic orientation of the substrate was $[1\bar{1}02]$ with a thickness of about 0.4 mm. Magnetic susceptibility measurements indicated a sharp superconducting transition at 32 K with a width of 1 K (upper frame of Fig. 1). The details of the growth process will be given elsewhere [15]. The transition temperature of our film is lower compared to thin films, obtained by *ex situ* annealing of the boron films (e.g., [16]). However, for a number of applications and for various basic studies, epitaxial films are necessary. The epitaxial growth seems to be very difficult to obtain in the *ex situ* process [17]. $T_c = 32$ K of our film is on the upper limit of what can be presently obtained without a high-pressure postanneal (24–34 K [17,18]). The MgB_2 film used in this paper has been characterized by four-circle x-ray diffraction. The c-axis of our film is tilted from the substrate normal by an angle of 77°, i.e., the film orientation is close to the a-axis orientation. However, within the experimental accuracy

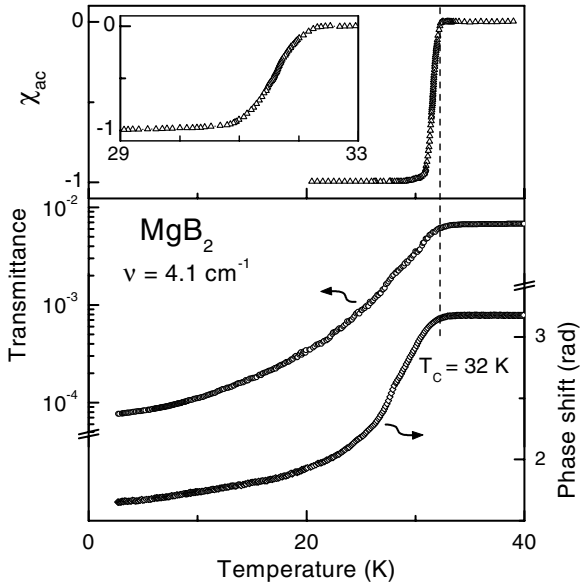

FIG. 1. Upper panel: temperature dependence of the magnetic susceptibility of MgB_2 film on Al_2O_3 substrate. The inset shows the data at about $T = T_c$ on an enlarged scale. Lower panel: temperature dependence of the transmittance at a fixed frequency $\nu = 4.1$ cm^{-1} (left scale) and temperature dependence of the phase shift at the same frequency (right scale).

of a few percent the conductivity measurements did not show any substantial anisotropy neither in the normal nor in the superconducting state.

The measurements in the submillimeter-wave range were performed using a coherent source spectrometer [19]. Four backward-wave oscillators (BWO's) have been employed as monochromatic and continuously tunable sources covering the frequency range from 4 to 30 cm^{-1}. The Mach-Zehnder interferometer arrangement has allowed measuring both the intensity and the phase shift of the wave transmitted through the MgB_2 film on the substrate. Using the Fresnel optical formulas for the complex transmission coefficient of the substrate-film system, the complex conductivity has been determined directly from the measured spectra. The optical parameters of the bare substrate were obtained in a separate experiment. In this work, we have measured the frequency spectra of the transmittance and the phase shift at several temperatures in the normal (above T_c) and in the superconducting states of MgB_2. In addition, we have also measured temperature dependences of these quantities at a fixed frequency (4.1 cm^{-1}) continuously from 2.7 to 60 K. A more detailed description of the experimental setup and of the data analysis is given in Refs. [13,19].

The lower frame of Fig. 1 represents the temperature dependence of the transmittance and the phase shift of the MgB_2 film at $\nu = 4.1$ cm^{-1}. Above the superconducting transition both quantities are almost temperature independent. This behavior is consistent with the absence of temperature dependence of the dc resistivity in MgB_2 in this temperature region [1]. The onset of the superconductivity is immediately reflected in the transmittance and phase shift. Both start to decrease below T_c, corresponding to an increase of σ_2 in the superconducting phase due to the Meissner effect.

Examples of the complex conductivity spectra, directly calculated from the frequency-dependent transmittance and phase shift, are shown in Fig. 2. The normal-state conductivity (35 K curve) demonstrates typical metallic behavior. The real part of the conductivity is essentially frequency independent, while the imaginary part is almost zero and exhibits a small linear increase for increasing frequencies. This indicates a Drude conductivity with a scattering rate above the measured frequency window. Simultaneous fitting of the σ_1 and σ_2 spectra with a Drude model gives an estimate for the scattering rate at 35 K: $1/2\pi\tau = 150^{+70}_{-50}$ cm^{-1}.

The transition into the superconducting state gives rise to significant changes in the spectra. σ_2 starts to diverge for $\nu \to 0$ (Fig. 2, upper frame). This divergence increases with decreasing temperature, reflecting a growth of the spectral weight of the superconducting condensate. The frequency dependence of σ_2 can be well described by the $1/\nu$ dependence, which corresponds to the δ function in σ_1 at $\nu = 0$ via the Kramers-Kronig relations. In the superconducting state a pronounced frequency dispersion arises in the σ_1 spectra as well (Fig. 2, lower frame). At low frequencies ($\nu < 9$ cm^{-1}), and starting from the

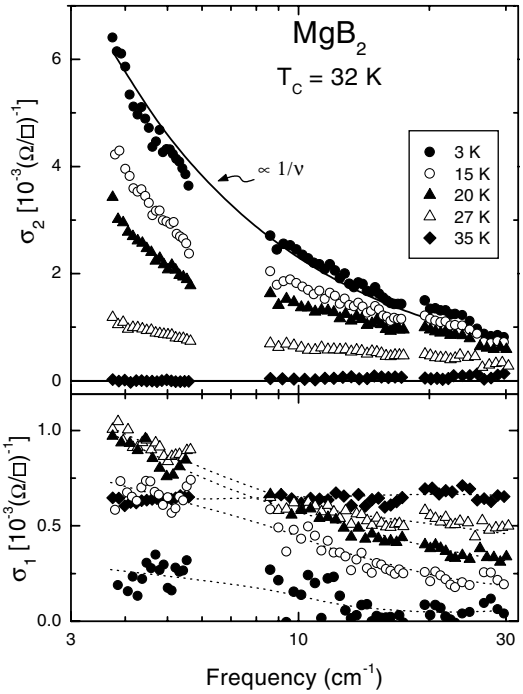

FIG. 2. Frequency dependence of the complex conductivity of MgB_2 film above and below T_c. Upper panel: imaginary part σ_2. The solid line represents the $\sigma_2 \propto 1/\nu$ dependence. Lower panel: real part σ_1. The lines are drawn to guide the eye. Scattering of the experimental points and the mismatch between different BWO's represent the experimental accuracy.

normal state, σ_1 initially increases (by approximately a factor of 1.5 at the lowest frequency) and then decreases, while at higher frequencies, $\nu > 9$ cm^{-1}, σ_1 monotonously decreases upon cooling. At the lowest temperatures ($\sim$3 K), σ_1 almost approximates zero at higher frequencies (within the experimental accuracy), indicating the absence of the normal carrier contribution to the electromagnetic response at $T \to 0$, and confirming the high quality of the film.

From the temperature evolution of the conductivity spectra it becomes clear that a maximum in the temperature dependence of σ_1 should exist below T_c and at low frequencies. The temperature dependencies of σ_1 and σ_2 for several frequencies are shown in Fig. 3. The temperature dependence of σ_1 for $\nu = 4.1$ cm^{-1} is calculated from the transmittance and phase-shift measurements, presented in Fig. 1. (For better representation the data for $\nu = 4.1$ cm^{-1} are shown in a separate frame.) The data in the two other frames were taken from the frequency spectra (Fig. 2). The thick lines in Fig. 3 show the weak-coupling BCS calculations for the frequencies indicated. Because the scattering rate $1/2\pi\tau = 150$ cm^{-1} has been determined from the normal-conducting state, the value of the energy gap remains the only free parameter for these calculations. We have chosen $\Delta(0) = 3.7$ meV so that the theoretical curves at the lowest temperatures match the experimental values of σ_2. The BCS curves do not fit the experimental points at intermediate temperatures, and we were not able to significantly improve the simultaneous fit of σ_1 and σ_2 data either by taking different ratios of $2\Delta/kT_c$, or by introducing a distribution of superconducting transition temperatures in the calculations.

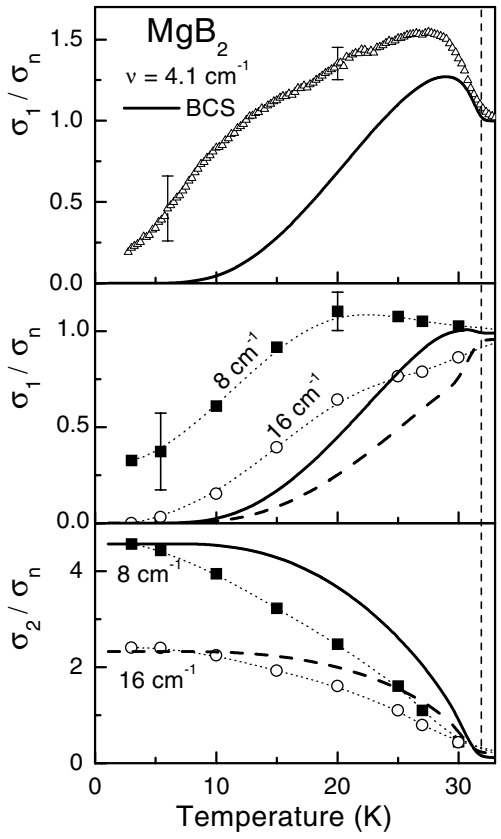

FIG. 3. Temperature dependence of the complex conductivity of MgB_2 film for several frequencies. Upper panel: σ_1 at 4.1 cm^{-1}. The solid line represents the BCS model calculation with $\Delta = 3.7$ meV, $1/2\pi\tau = 150$ cm^{-1}. Lower panels: temperature dependencies of the real (middle) and imaginary (bottom) parts of the complex conductivity at 8.2 cm^{-1} (solid squares) and at 16 cm^{-1} (open circles). The thick lines represent the BCS calculations with the same parameters as in the upper panel; solid line: $\nu = 8.2$ cm^{-1}, dashed line: $\nu = 16$ cm^{-1}. The thin dotted lines are drawn to guide the eye. The vertical line indicates T_c. The error bars are estimated from the scattering of the experimental points in the frequency spectra (Fig. 2).

The peak in the temperature dependence of σ_1 vanishes at frequencies above 9 cm^{-1}, and the temperature dependence of σ_1 at higher frequencies basically follows the behavior shown in Fig. 3 for $\nu = 16$ cm^{-1}. The observed peak in $\sigma_1(T)$ is reminiscent of the coherence peak, predicted for a BCS superconductor in the dirty limit. The measured $\sigma_1(T)$ dependencies for all frequencies are higher than the BCS calculations. This disagreement could be caused by an additional absorption. It is difficult to say whether this absorption is of intrinsic or extrinsic origin. However, the absorption tends to disappear at $T \to 0$ (see also the lower panel of Fig. 2), which seems to be in favor of an intrinsic nature of the absorption.

The temperature dependence of the imaginary part of the complex conductivity (Fig. 3, lower panel) deviates significantly from the BCS curves. Qualitatively the same deviations from the BCS calculations have been found for all measured frequencies: the slope of the experimental $\sigma_2(T)$ curves is more gradual at temperatures just above T_c, and at $T \to 0$ it is steeper than the BCS prediction. Since the superconducting penetration depth is directly connected to the imaginary part of conductivity via $\lambda = (\mu_0\omega\sigma_2)^{-1/2}$ (μ_0 is the vacuum permeability and $\omega = 2\pi\nu$ is the angular frequency), for further discussion we focus on the temperature dependence of the penetration depth (Fig. 4).

Figure 4 compares the penetration depth in MgB_2 with the predictions of different models. The experimental data (open triangles) were calculated from the temperature dependence of the transmittance and phase shift measured at $\nu = 4.1$ cm^{-1} (Fig. 1). The solid line represents the weak-coupling BCS calculations with the parameters used in Fig. 3. The dotted line shows the result of the two-fluid model $[1 - (T/T_c)^4]$. The dashed line represents the $[1 - (T/T_c)^2]$ dependence. The first two dependencies reproduce the temperature variation of the penetration depth in conventional superconductors [20], and the last one often reasonably fits the experimental penetration depth in the high-T_c cuprates [21]. The experimental data in Fig. 4 clearly deviate from all these model curves in the whole temperature range below T_c.

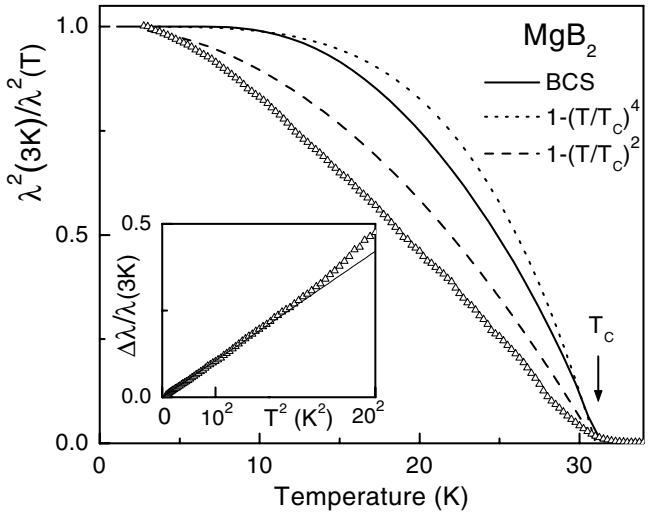

FIG. 4. Temperature dependence of the low-frequency penetration depth of MgB_2 film. Symbols: experimental data as obtained from the temperature-dependent transmittance and phase shift shown in Fig. 1. The lines represent various model calculations, solid: weak-coupling BCS, dotted: two-fluid $[1 - (T/T_c)^4]$; dashed: $[1 - (T/T_c)^2]$. The inset shows the temperature variation of the penetration depth below 20 K as a function of T^2.

The inset of Fig. 4 shows the temperature variation of the penetration depth as a function of T^2 and at low temperatures. The experimental points below approximately 15 K closely follow a straight line, indicating that a T^2 behavior is a good approximation to the low-temperature data (in agreement with the muon spin-rotation measurements [9]). The power-law dependence of the penetration depth in the zero-temperature limit was observed in various high-T_c superconductors and interpreted as evidence for the existence of nodes in the gap function. However, in the case of a strongly anisotropic s-wave energy gap the transition to the BCS-like exponential behavior may take place at even lower temperatures than obtained in this paper ($\sim$2.7 K). Therefore, the results of Fig. 4 suggest a strong gap anisotropy, or may even indicate the existence of nodes in the gap function.

In conclusion, we have measured the complex conductivity of MgB_2 film in the frequency range $4 < \nu < 30$ cm^{-1} and for temperatures $2.7 < T < 300$ K. The temperature dependence of the real part of the low-frequency conductivity shows a peak below the superconducting transition, which qualitatively agrees with the predictions of the BCS theory. However, detailed comparison of the complex conductivity with the BCS model calculations shows significant discrepancies between the experiment and the theory. The temperature dependence of the penetration depth is consistent with the $\delta\lambda \propto T^2$ behavior below $\sim$15 K, which implies significant anisotropy in the gap function.

We thank S. Six, Ch. Schneider, and G. Hammerl for the help in film characterization. This work was supported by the BMBF via Contract No. 13N6917/0-EKM. A. V. P. acknowledges partial support by SFB 484.

*Corresponding author.
Email address: Andrei.Pimenov@Physik.Uni-Augsburg.DE

[1] J. Nagamatsu *et al.,* Nature (London) **410**, 63 (2001).
[2] See, e.g., J. E. Hirsch and F. Marsiglio, cond-mat/0102479; A. Y. Liu *et al.,* cond-mat/0103570; S. V. Shulga *et al.,* cond-mat/0103154; J. M. An and W. E. Pickett, Phys. Rev. Lett. **86**, 4366 (2001); Y. Kong *et al.,* Phys. Rev. B **64**, 020501 (2001).
[3] S. L. Bud'ko *et al.,* Phys. Rev. Lett. **86**, 1877 (2001).
[4] G. Karapetrov *et al.,* Phys. Rev. Lett. **86**, 4374 (2001); A. Sharoni *et al.,* Phys. Rev. B **63**, 220508 (2001); H. Schmidt *et al.,* Phys. Rev. B **63**, 220504 (2001).
[5] E. Bascones and F. Guinea, cond-mat/0103190.
[6] T. Takahashi *et al.,* Phys. Rev. Lett. **86**, 4915 (2001).
[7] S. Tsuda *et al.,* cond-mat/0104489.
[8] H. Kotegawa *et al.,* cond-mat/0102334.
[9] C. Panagopoulos *et al.,* cond-mat/0103060.
[10] S. L. Li *et al.,* cond-mat/0103032.
[11] B. Gorshunov *et al.,* Eur. Phys. J. B **21**, 159 (2001).
[12] J. H. Jung *et al.,* cond-mat/0105180.
[13] A. V. Pronin *et al.,* Phys. Rev. B **57**, 14 416 (1998); A. Pimenov *et al.,* Phys. Rev. B **59**, 4390 (1999); A. Pimenov *et al.,* Phys. Rev. B **62**, 9822 (2000).
[14] V. S. Nozdrin *et al.,* Tech. Phys. Lett. **22**, 996 (1996).
[15] S. I. Krasnosvobodtsev *et al.* (to be published).
[16] W. N. Kang *et al.,* Science **292**, 1521 (2001).
[17] H. M. Christen *et al.,* cond-mat/0103478; X. H. Zeng *et al.,* cond-mat/0105080.
[18] D. H. A. Blank *et al.,* cond-mat/0103543.
[19] G. V. Kozlov and A. A. Volkov in *Millimeter and Submillimeter Wave Spectroscopy of Solids,* edited by G. Grüner (Springer, Berlin, 1998).
[20] M. Tinkham, *Introduction to Superconductivity* (McGraw-Hill, New York, 1975).
[21] D. A. Bonn and W. N. Hardy, in *Physical Properties of High Temperature Superconductors V,* edited by D. M. Ginsberg (World Scientific, Singapore, 1996), p. 7.